Journal of Cerebral Blood Flow & Metabolism (2012) 32, 1496–1507

www.jcbfm.com

Imaging of perfusion, angiogenesis, and tissue elasticity after stroke

Abraham Martín[1,3], Emilie Macé[2], Raphael Boisgard[1], Gabriel Montaldo[2], Benoit Thézé[1], Mickael Tanter[2] and Bertrand Tavitian[1]

[1]*Inserm U1023, Université Paris Sud, CEA, DSV, I2BM, Orsay, France;* [2]*Institut Lanvegin, ESCPI, Paris, France*

Blood flow interruption in a cerebral artery causes brain ischemia and induces dramatic changes of perfusion and metabolism in the corresponding territory. We performed in parallel positron emission tomography (PET) with [^{15}O]H_2O, single photon emission computed tomography (SPECT) with [^{99m}Tc]hexamethylpropylene-amino-oxime ([^{99m}Tc]HMPAO) and ultrasonic ultrafast shear wave imaging (SWI) during, immediately after, and 1, 2, 4, and 7 days after middle cerebral artery occlusion (MCAO) in rats. Positron emission tomography and SPECT showed initial hypoperfusion followed by recovery at immediate reperfusion, hypoperfusion at day 1, and hyperperfusion at days 4 to 7. Hyperperfusion interested the whole brain, including nonischemic areas. Immunohistochemical analysis indicated active angiogenesis at days 2 to 7, strongly suggestive that hyperperfusion was supported by an increase in microvessel density in both brain hemispheres after ischemia. The SWI detected elastic changes of cerebral tissue in the ischemic area as early as day 1 after MCAO appearing as a softening of cerebral tissue whose local internal elasticity decreased continuously from day 1 to 7. Taken together, these results suggest that hyperperfusion after cerebral ischemia is due to formation of neovessels, and indicate that brain softening is an early and continuous process. The SWI is a promising novel imaging method for monitoring the evolution of cerebral ischemia over time in animals.
Journal of Cerebral Blood Flow & Metabolism (2012) **32,** 1496–1507; doi:10.1038/jcbfm.2012.49; published online 11 April 2012

Keywords: middle cerebral artery occlusion; PET; shear wave imaging; SPECT; stroke; ultrasound

Introduction

Stroke, a leading cause of death worldwide (López *et al*, 2006), was first recognized as a separate clinical and pathological entity in the early 1820s by Rostan (1823) who called it *ramollissement du cerveau*, meaning 'softening of the brain' in French. Soon after, Abercrombie (1828) linked *ramollissement* to the failure of arterial circulation in a cerebral blood vessel. These descriptions of stroke pathogenesis remain valid almost two centuries later. In four out of five stroke cases, the interruption of blood flow in a cerebral vessel leads to tissular ischemia and loss of function in the vascular territory. Spontaneous or therapeutic (Khatri *et al*, 2009) reestablishment of blood flow conditions the functional recovery, else the loss of function becomes permanent and cerebral softening of the tissue, the hallmark of stroke at autopsy, eventually appears.

Much more is known today about the cellular reactions after stroke than was at the time of Rostan and Abercrombie, e.g., the roles of active growth of blood vessels (Plate, 1999), angiogenesis (Lin *et al*, 2008), and inflammation (Brea *et al*, 2009; Thiel and Heiss, 2011). However, accurate descriptions of the cerebral blood flow (CBF) changes in relationship with tissue softening, of how the metabolic demand of the tissue is compensated for or not, of the mechanisms leading to irreversible cerebral softening or, vice versa, to functional cerebral recovery after stroke, are still incomplete.

Because tissue responses after ischemic stroke are highly dynamic, imaging methods are ideal to provide longitudinal data (Latchaw *et al*, 2003) and to inform on the natural evolution of ischemic stroke and on the effect of candidate treatments (Martín *et al*, 2010, 2011). Presently, imaging techniques to assess cerebral perfusion after stroke include positron emission tomography (PET), single photon emission computed tomography (SPECT), magnetic

Correspondence: Professor B Tavitian, Inserm U1023, CEA, 4 place du géneral Leclerc, Orsay 91400, France.
E-mail: bertrand.tavitian@cea.fr
[3]Present address: Molecular Imaging Unit, CICbiomaGUNE, San Sebastián, Guipuzcoa, Spain.
This study was supported by the sixth FW EU grants EMIL (LSHC-CT-2004-503569) and DiMI (LSHB-CT-2005-512146).
Received 24 November 2011; revised 14 February 2012; accepted 9 March 2012; published online 11 April 2012

resonance imaging, computed X-ray tomography, and ultrasound (Wintermark, 2005). Concerning PET, [^{15}O]H_2O has been widely used to measure CBF in patients (Heiss, 2000) as well as in experimental middle cerebral artery occlusion (MCAO) in baboons (Pappata *et al*, 1993) and in cats (Heiss *et al*, 1994). The SPECT using [^{99m}Tc]hexamethylpropylene-amino-oxime ([^{99m}Tc]HMPAO) is also a well-established imaging method to measure relative CBF in acute cerebral ischemia. The [^{99m}Tc]HMPAO has been used to predict the risk of hemorrhagic transformation (Ueda *et al*, 1994), severe edema (Umemura *et al*, 2000), and spontaneous reperfusion after acute cerebral ischemia (Bowler *et al*, 1998). Recently, novel ultrasonographic imaging techniques have augmented the repertoire of cerebral imaging techniques for small animals (Macé *et al*, 2011). Shear wave imaging (SWI) offers quantitative assessment of the viscoelasticity of tissues (Bercoff *et al*, 2004) and detects abnormal biomechanical features in pathologies affecting the breast, liver (Tanter *et al*, 2008; Muller *et al*, 2009), and arterial walls (Couade *et al*, 2010).

The purpose of the present study was to investigate the time course of changes in perfusion, CBF, and tissue elasticity after experimental ischemia in the rat. In particular, we were interested in (1) the kinetics of early vascular changes and (2) determining whether tissue softening is an early phenomenon or the end point of the natural evolution after ischemic stroke. The answer to these questions may have some practical importance as they could help to better understand the reversibility or irreversibility of the cerebral lesions after ischemia and perhaps to better define the initial time windows for therapeutic intervention. Multimodal imaging using PET, SPECT, and ultrafast ultrasound SWI imaging was applied to derive angiographic, perfusion, and elasticity data related to the natural evolution of a 2-hour MCAO in rats. Examinations at identical time points and quantitative analysis of the data in groups of animals allowed statistical comparisons.

Materials and methods

Animals and Surgery

Adult male Sprague-Dawley rats (300 g body weight; Charles River, St-Germain-sur-l'Arbresle, France) ($n=52$) were used. Animal studies were approved by the animal ethics committee of Institut d'Imagerie Biomédicale (I^{2}BM) and conducted in accordance with Directive 2010/63/EU of the European Parliament. Transient focal ischemia was produced by a 2-hour intraluminal MCAO followed by reperfusion as described elsewhere (Rojas *et al*, 2011). Briefly, rats were anesthetized with 4% isofluorane in 100% O_2 and a 2.6-cm length of 4-0 monofilament nylon suture was introduced into the right external carotid artery up to the level where the middle cerebral artery (MCA) branches out. The ipsilateral common carotid artery was also ligated to reduce the collateral blood flow and animals were sutured and placed in their cages with free access to water and food. After 2 hours, the animals were reanesthetized, the filament was removed and the clip on the common carotid artery was released to allow reperfusion. The contralateral common carotid artery was not occluded during ischemic process and no damage was observed in the contralateral hemisphere after reperfusion. Animals were studied at occlusion ($n=5$) and at 1 hour ($n=4$), 1 ($n=9$), 2 ($n=9$), 4 ($n=10$), and 7 ($n=9$) days after reperfusion onset. Nonoperated animals were used as controls ($n=6$).

Thirty-two animals were subjected to PET and SPECT studies at occlusion ($n=5$) and at 1 hour ($n=4$), and 1 ($n=5$), 2 ($n=4$), 4 ($n=6$), and 7 ($n=5$) days after reperfusion onset. Non MCAO-operated animals were used as controls ($n=3$). Animals were killed at the end of each PET/SPECT study to perform immunohistochemistry.

Twenty animals were subjected to B-mode and SWI ultrasound imaging at 1 ($n=4$), 2 ($n=5$), 4 ($n=4$), and 7 ($n=4$) days after induction of cerebral ischemia. Non MCAO-operated rats were used as controls ($n=3$). Ultrasound imaging was performed only once in each animal and animals were killed at the end of the ultrasound imaging session.

Radiochemistry

The [^{99m}Tc]-HMPAO was prepared using the commercial kit Cerestab (GE Healthcare, Vélizy, France) following provider's recommendations for preparation and quality control. [^{15}O]H_2O was synthesized by standard procedures from cyclotron-produced [^{15}O]oxygen sterilized by filtration on a 0.22-μm Millipore filter (Millipore, Molsheim, France).

Single Photon Emission Computed Tomography Scans and Data Acquisition

Single photon emission tomography studies were performed in rats anesthetized with 4% isofluorane and maintained by 2% to 2.5% of isofluorane in 100% O_2. Single photon emission computed tomography imaging was performed on a Gamma Imager (Biospace, Paris, France) during 60 minutes after intravenous injection of 74.5 MBq of [^{99m}Tc]HMPAO.

Positron Emission Tomography Scans and Data Acquisition

Positron emission tomography was performed immediately after SPECT. Rat's head was placed in a stereotaxic frame and PET images acquired on a Concorde Focus 220 camera (Siemens Medical Solutions, Knoxville, TN, USA) during 5 minutes after intravenous injection of 200 MBq of [^{15}O]H_2O. The attenuation correction factors were calculated from the emission map, emission sinograms were normalized, corrected for attenuation and radioactivity decay, and reconstructed using FORE and OSEM 2D (16 subsets and 4 iterations).

Single Photon Emission Computed Tomography and Positron Emission Tomography Image Analysis

The SPECT and PET images were coregistered to a T2 magnetic resonance imaging rat brain template (Schweinhardt *et al*, 2003) using Anatomist software (http://brainvisa.info). Regions of interest (ROIs) were manually defined in the entire ipsilateral hemisphere containing the territory irrigated by the MCA and then mirrored to the homologous contralateral hemisphere. The mean value and the standard deviation of each ROI in the PET images were measured using the Anatomist software. For PET, the summed uptake during the first 25 seconds of acquisition was expressed in percent of injected dose per mL of tissue (ID/g). For SPECT, uptake at 60 minutes of acquisition was expressed in arbitrary units.

Ultrafast Ultrasound Scans

B-mode and Shear Wave (SWI) ultrasound imaging were performed at 1 ($n=4$), 2 ($n=5$), 4 ($n=4$), and 7 ($n=4$) days after induction of cerebral ischemia and in nonoperated rats used as controls ($n=3$). The strong attenuation of ultrasound by the skull precludes transcranial imaging of the brain. As a result, the overlying bone must be partially removed before the imaging session. Animals were anesthetized as above and placed in a stereotaxic frame. The skin and periosteum were removed to expose the top of the skull and the *temporalis* muscle was detached from the bone on both sides to expose the temporal part of the skull. A cranial window, 8 mm long in the sagittal direction, −4 mm to +4 mm from bregma point, and 10 mm wide in the coronal direction was opened using a 1.4-mm drill. The bone fragment was removed carefully to leave the dura matter intact and a 3-mm ridge of dental cement was cast around the cranial window filled with an isotonic aqueous solution of xantam gum (0.3%). Xantam gum increased the viscosity of water and ensured proper acoustic coupling. The complete surgical procedure lasted ~2 hours and was immediately followed by acquisition of the ultrasound imaging scans. The ultrasound probe was set above the brain in the coronal plane and aligned with the bregma point. Adjacent coronal acquisitions were performed by motor-controlled movement of the probe in 400 μm steps from β +3 to β +3 mm. An 8-MHz central frequency linear array (array pitch 0.2 mm) was used for SWI whereas a 15-MHz central frequency linear array (array pitch 0.125 mm) (both from Vermon, Tours, France) was used for B-mode Imaging. The probe was controlled by an ultrafast ultrasound scanner (Aixplorer V2 prototype; Supersonic Imagine, Aix-en-Provence, France) programmed with custom transmit/receive ultrasonic sequences.

Shear Wave Imaging Data Acquisition and Image Analysis: The SWI sequence has been described in detail in Macé *et al* (2011). Briefly, after a shear wave was generated with a 90-μs ultrasonic beam focused supersonically (4 mm in depth), 70 ultrafast images (compound images, 3 angles: −8°, 0°, 8°) were acquired at 5 kHz. For each coronal plane, 10 SWI acquisitions were performed at 10 different shear wave source locations (duration of each acquisition ca. 10 ms, total acquisition time for one plane ca. 100 ms). Postprocessing with a dedicated algorithm calculated for each pixel the time of flight of the shear wave (i.e., the inverse of the shear wave speed in s/m), yielding an elasticity map of the cerebral tissue. For each animal, ROIs were defined by segmentation of the ischemic lesion based on its hyperechogenicity in the B-mode, i.e., pixels with a hyperechogenicity >15 dB with respect to the corresponding pixel in the opposite hemisphere were considered to be inside the ischemic area. The ROIs were then mirrored to the hemisphere contralateral to the lesion. In control animals, ROIs were defined as the whole volume of the right hemisphere (ipsi) or left hemisphere (contra). For each ROI, the reciprocal of the mean time of flight was taken as the mean shear wave velocity and expressed in m/s.

Immunohistochemistry

Immunohistochemistry staining was performed after PET/SPECT imaging. Animals were terminally anesthetized, killed by decapitation; the brain was removed, frozen and cut in 5-μm-thick sections in a cryostat. Sections were fixed in Acetone (−20°C) during 2 minutes, washed with phosphate-buffered saline (PBS) and saturated with a solution of BSA 5%/Tween 0.5% in PBS during 15 minutes at room temperature, and incubated during 1 hour at room temperature with mouse anti-rat CD31 (Pharmingen, Le Pont-de-Claix, France, 1:50) in BSA 5%/Tween 0.5% in PBS. Sections were washed (3 × 10 minutes) in PBS and incubated for 1 hour at room temperature with Alexa Fluor 594 nm rat anti-mouse IgG (Molecular Probes, Life Technologies, Villebon-sur-Yvette, France, 1:1,000) in BSA 5%/Tween 0.5% in PBS, washed again (3 × 10 minutes) in PBS, and mounted with a DAPI Prolong Antifade kit (Molecular Probes). Standardized images acquisition was performed with an Axio Observer Z1 (Zeiss, Le Pecq, France) equipped with a motorized stage.

Vessel Counts

The number of CD31-positive vessels within the ischemic area was assessed by counting manually the number of stained vessels in 10 fields (0.57 mm × 0.57 mm, totaling an area of 3.249 mm^2) in the lesioned side and the non-ischemic side. Five fields were randomly placed in the ischemic area and five fields placed in the region surrounding to the lesion.

Statistical Analyses

Statistical differences were analyzed using one-way analysis of variance, Bonferroni's multiple comparison tests for *post-hoc* analysis, and linear regression for the correlation between [^{99m}Tc]HMPAO and [^{15}O]H_2O. Statistical analyses were performed with *GraphPad Prism* software (GraphPad Software, La Jolla, CA, USA).

Results

Perfusion, angiogenesis, and tissue elasticity were explored by imaging after a 2-hour MCAO in rats. All the images were quantified in standard units, i.e., percent of the injected dose per volume tissue for PET and SPECT, m/s for elastometry and number of positively stained vessels per surface area for CD31 immunohistochemistry. Hence, the measurements made at different time points in ROIs of the ischemic area and the mirror contralateral area can be compared directly with the measurements made in control animals and images with normalized color scales illustrate the evolution of the signal over time (Figure 1).

[^{15}O]H_2O Positron Emission Tomography and [^{99m}Tc]Hexamethylpropylene-Amino-Oxime Single Photon Emission Computed Tomography

Cerebral perfusion was evaluated using [^{15}O]H_2O PET and [^{99m}Tc]HMPAO SPECT before, during, and at 1, 2, 4, and 7 days after MCAO (Figure 1). [^{15}O]H_2O PET and [^{99m}Tc]HMPAO SPECT signals were significantly lower (−50%) in the cerebral territory of the occluded MCA during occlusion than in the same region of sham-operated animals. During early reperfusion, immediately after the release of MCAO, PET and SPECT signals returned to quasi-normal values. One day after reperfusion, however, [^{15}O]H_2O PET and [^{99m}Tc]HMPAO SPECT signals dropped again to 60% that of control animals. Subsequently, [^{15}O]H_2O PET and [^{99m}Tc]HMPAO SPECT signals rose steadily, reaching control values at day 2 after ischemia and continuously rising thereafter. Perfusion values measured by [^{15}O]H_2O PET and [^{99m}Tc]HMPAO SPECT were higher than in control animals by day 4, although the difference did not reach statistical significance at that time. By day 7, [^{15}O]H_2O PET and [^{99m}Tc]HMPAO SPECT signals were twofold higher in the occluded MCA territory than in controls, and the differences were statistically significant ($P<0.001$) (Figures 2A and 2C).

Interestingly, changes in [^{15}O]H_2O PET and [^{99m}Tc]HMPAO SPECT signals were also observed in the contralateral, nonischemic area. Contralateral perfusion was reduced by 20% during MCAO, returned to control values during reperfusion, and dropped again to 75% to 80% of control at day 1. Afterwards, [^{15}O]H_2O PET and [^{99m}Tc]HMPAO SPECT contralateral signals increased in parallel to the ipsilateral region, reaching values of control animals at days 2 to 4 and twofold higher than control values at day 7. The increase of [^{15}O]H_2O PET signal in the contralateral hemisphere with respect to that of the controls was significant ($P<0.001$) at day 7 (Figure 2B), while the increase in the uptake of [^{99m}Tc]HMPAO, with respect to that of control animal, was detected not statistically significant at day 4 and became highly significant ($P<0.001$) by day 7 (Figure 2D).

As a consequence, the ratio of perfusion values in the ipsilateral (occluded MCA) over contralateral (nonoccluded MCA) areas presented the same 'camel-shaped' time course as that recorded in the MCAO territory: during MCAO, perfusion in the ischemic area was twofold lower than in the contralateral area, rose to 85% of the contralateral values on reperfusion, dropped again to 70% to 75% of contralateral at day 1, then increased to a ratio of one (i.e., similar perfusion values in the territory of obstructed and nonobstructed MCA) at days 4 and 7.

Linear regression analysis showed a significant positive correlation ($r^2=0.7218$, $P<0.001$) between the ^{15}O-H_2O PET and [^{99}Tc]HMPAO SPECT signals measured sequentially in the same animals at all time points (Figure 3), indicating that the measurement of the time course of brain perfusion changes after cerebral ischemia was independent of the imaging technique.

Time Course of Vessel Angiogenesis After Cerebral Ischemia

The formation of new vessels after ischemia was explored by immunofluorescent staining for CD31 (PECAM-1) a 130-kDa glycoprotein constitutively expressed by endothelial cells, in the cortical and subcortical areas of the brain parenchyma after cerebral ischemia and compared with that of control brains (Figure 4A). Interestingly, CD31 staining at day 1 after MCAO showed similar density and distribution as in control animals (Figures 4B and 4C). In contrast, at day 2, the density of CD31-positive vessels increased in the territory of the MCA (Figure 4D) and further increased at days 4 and 7. At day 7 after cerebral ischemia, both sides of the brain showed increased CD31 staining over controls, especially in the cerebral cortex (Figure 4E). The number of CD31-stained vessels per mm^2 in representative sections of controls and at days 1, 2, 4, and 7 after MCAO showed a similar time course profile as the one observed for [^{15}O]H_2O PET and [^{99m}Tc]HMPAO. In the MCAO territory, a nonsignificant decrease of CD31-positive vessel density at day 1 was followed by an increase at days 2 to 4, peaking at day 7 after reperfusion. Quantitative analysis indicated a significant increase of CD31-positive vessels at day 4 ($P<0.01$) and day 7 ($P<0.001$) when compared with control (Figure 5). Moreover, at day 7 an increase in CD31-positive vessel density was observed in the cerebral hemisphere contralateral to the occluded MCA territory, and was statistically significant with respect to control animals ($P<0.01$) after cerebral ischemia. However, the ipsilateral-to-contralateral ratio remained higher than unity from day 2 onwards, indicating a higher density of CD31 positivity in the MCAO territory.

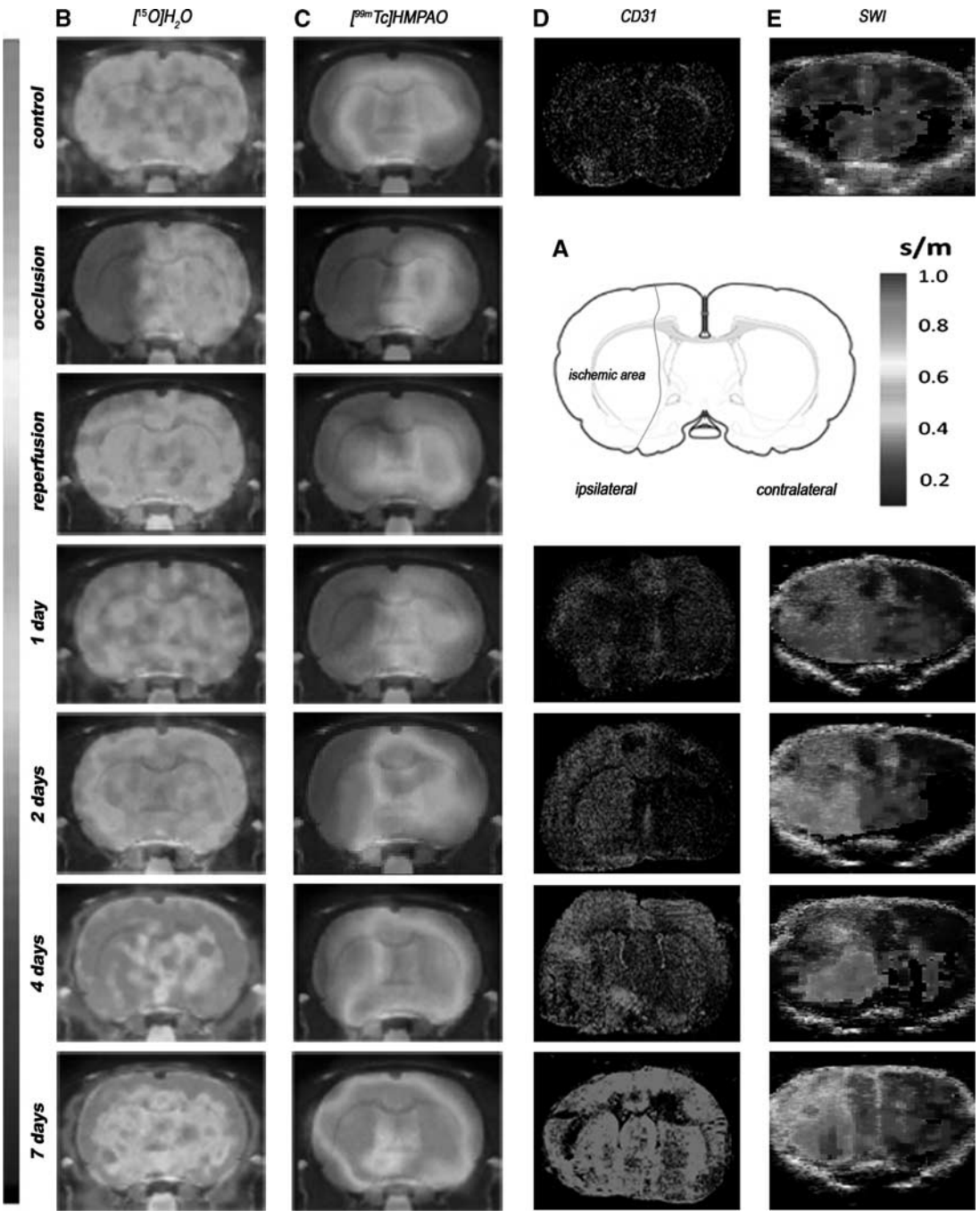

Figure 1 Serial images of $[^{15}O]H_2O$ PET, $[^{99m}Tc]$HMPAO SPECT, CD31 immunohistochemistry, and shear wave imaging (SWI) during occlusion, early reperfusion and at day 1, day 2, day 4, and day 7 after middle cerebral artery occlusion (MCAO). (**A**) Rat brain section showing a representative ischemic area after MCAO. (**B**) PET, (**C**) SPECT, (**D**) CD31, and (**E**) SWI images. Panels **B** and **C** are coregistered with a magnetic resonance imaging (MRI) (T1) rat template; panel **E** is coregistered with B-mode images. PET, positron emission tomography; SPECT, single photon emission computed tomography; $[^{99m}Tc]$HMPAO, $[^{99m}Tc]$hexamethyl-propylene-amino-oxime.

Shear Wave Imaging After Cerebral Ischemia

Tissue elasticity was assessed by measuring the wave speed of shear waves with ultrafast ultrasound imaging in the brains of control animals and at days 1, 2, 4, and 7 after induction of cerebral ischemia (Figure 6). Shear wave speed in the territory of the occluded MCA varied from 3.5 m/s in normal cerebral tissue to 2 m/s at day 7 after the onset of cerebral ischemia. The decrease in the shear wave speed over time evidence the decrease of tissue elasticity (i.e., softening of tissue) as a result of

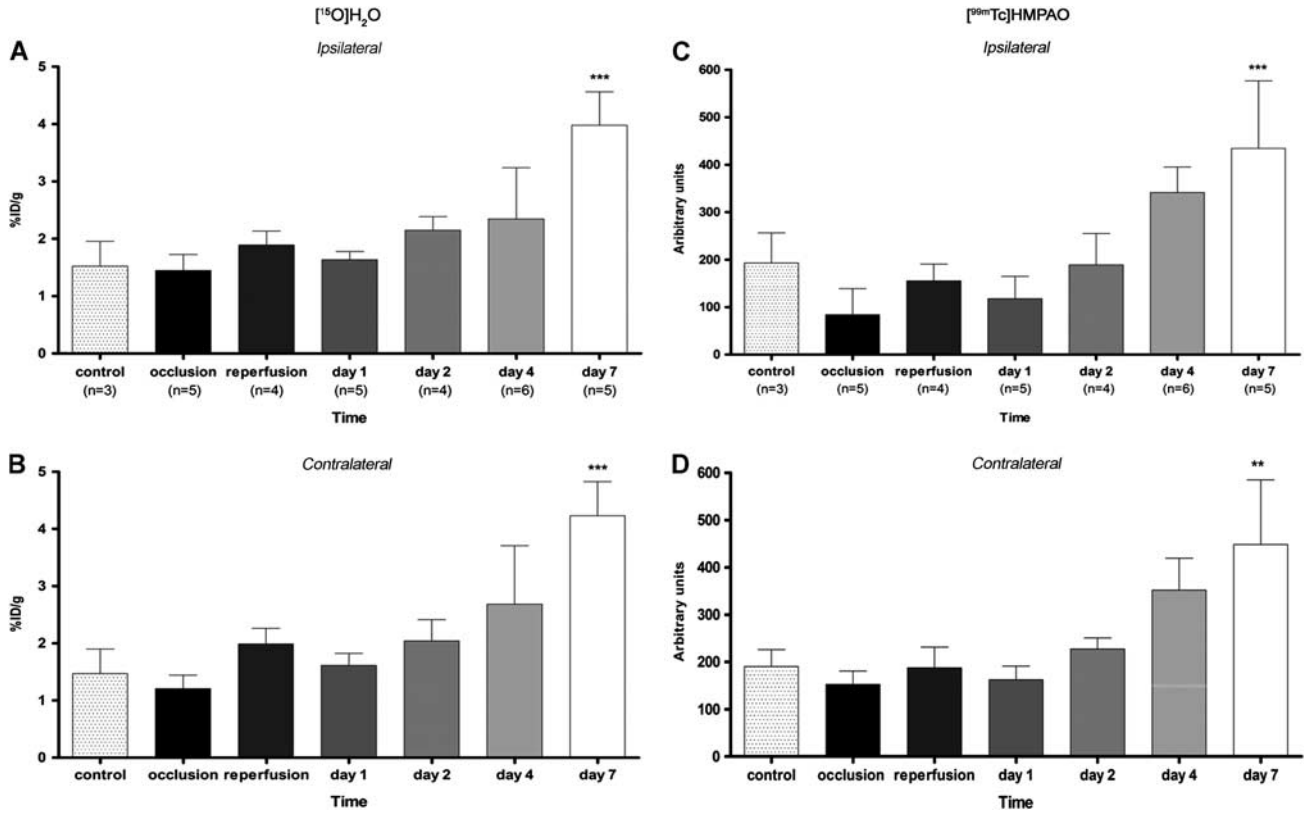

Figure 2 Time course of the $[^{15}O]H_2O$ PET and $[^{99m}Tc]$HMPAO SPECT signals during and after ischemia in the area ipsilateral (**A**, **C**) and contralateral (**B**, **D**) to middle cerebral artery occlusion (MCAO). Statistically different from control: $^{**}P < 0.01$, $^{***}P < 0.001$. ID, injected dose; PET, positron emission tomography; SPECT, single photon emission computed tomography; $[^{99m}Tc]$HMPAO, $[^{99m}Tc]$hexamethylpropylene-amino-oxime.

cerebral tissue damage. In the MCAO territory, the shear wave speed decreased continuously from day 1 onwards in a linear manner. Shear wave speed was significantly lower than in control animals at day 2 ($P<0.05$), day 4 ($P<0.01$), and day 7 ($P<0.001$) after reperfusion. In the contralateral hemisphere to the occluded MCA territory, there was no evidence for changes of elasticity in cerebral tissue at any time point after ischemia. As a consequence, the ratio of shear wave speed values in the ipsilateral over contralateral areas presented the same profile as that recorded in the MCAO territory: a progressive decrease in the shear wave speed indicating softening of the ischemic tissue.

Discussion

Ischemic stroke is due to the impairment of CBF and leads ultimately to the transformation of cerebral tissue into a soft and disorganized material. Clinical observations have emphasized the importance for functional recovery of increased blood flow (Treger *et al*, 2005) and new vessel formation (Allen, 1984; Granger *et al*, 1992). Thrombolysis is often curative if performed during the first hours after blood flow interruption, but increases the risk of cerebral hemorrhages afterwards (Singer *et al*, 2008). Little is known however on the time course of brain tissue softening after stroke and how it relates to changes in cerebral tissue perfusion, even though understanding the time course of these critical postischemic changes could likely provide guidance for therapeutic strategies. Such studies are difficult to implement in patients where critical care is required but can be performed in animal models mimicking ischemic stroke (Liu and McCullough, 2011). The progression from ischemic injury to infarct after MCAO has been studied *ex vivo* at the histological and ultrastructural level in rats (Garcia *et al*, 1993, 1997). Here, we measured in parallel tissue perfusion and softness, using *in-vivo* imaging procedures and *ex-vivo* immunohistochemistry, after a transient MCAO in rats.

Vascular Response After Middle Cerebral Artery Occlusion : Perfusion, Blood Flow, and Angiogenesis

Positron emission tomography with $[^{15}O]H_2O$ is a robust and well-validated imaging technique to study cerebral perfusion in acute stroke (Heiss,

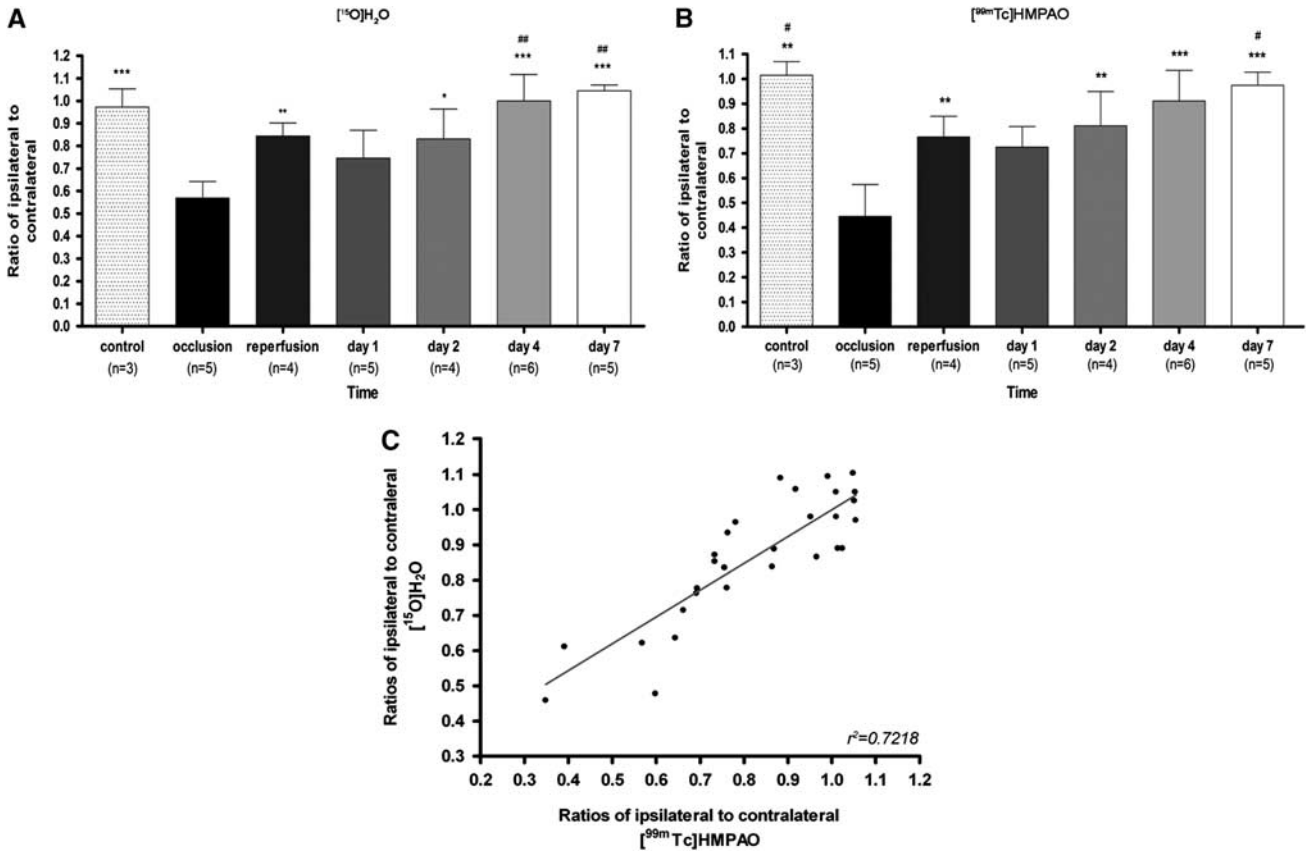

Figure 3 Time course of the ipsilateral to contralateral [^{15}O]H_2O PET (**A**) and [^{99m}Tc] HMPAO SPECT (**B**) signal ratios during and after ischemia. (**C**) Linear regression analysis showing the correlation between the [^{15}O]H_2O PET and [^{99m}Tc]HMPAO SPECT signal ratios ($P < 0.001$); each point is from an individual animal. Statistically different from ratio during occlusion: $^{*}P < 0.05$, $^{**}P < 0.01$, $^{***}P < 0.001$. Statistically different from ratio at day 1: $^{\#}P < 0.05$, $^{\#\#}P < 0.01$. PET, positron emission tomography; SPECT, single photon emission computed tomography; [^{99m}Tc]HMPAO, [^{99m}Tc]hexamethylpropylene-amino-oxime.

2000), but the availability of [^{15}O]H_2O is rare in routine clinical settings. Single photon emission computed tomography with [^{99m}Tc]HMPAO is more widely available for clinical studies (Brea *et al*, 2009) although only one *ex-vivo* autoradiographic study was reported in rats (Bullock *et al*, 1990). The present study is the first to evaluate cerebral perfusion *in vivo* using [^{99m}Tc]HMPAO in the MCAO model. Interestingly, [^{99m}Tc]HMPAO SPECT and [^{15}O]H_2O PET showed basically the same time course during and after MCAO, i.e., (1) a reduction by half during MCAO reflecting the interruption of blood flow, (2) a return to subnormal values during immediate reperfusion, followed by (3) a secondary decrease to roughly two thirds of the initial values at day 1, and (4) a steady increase thereafter leading to supernormal values by days 4 to 7. Positron emission tomography and SPECT showed only slight differences. Early immediate reperfusion was found relatively smaller in the lesioned area with SPECT than with PET, and SPECT showed higher relative values than [^{15}O]H_2O PET at day 4. Both techniques measure cerebral perfusion in different ways: [^{15}O]H_2O PET measures the transport of water through tissue in the first half-minute after a bolus intravenous injection, while the SPECT signal is due to the accumulation of a hydrophilic metabolite of [^{99m}Tc]HMPAO trapped in the parenchyma and is measured 1 hour after administration of the tracer (Sperling and Lassen, 1993). The chemical conversion step required to build-up the contrast with [^{99m}Tc]HMPAO could lead to overestimating cerebral perfusion after ischemia (Kuwabara *et al*, 1996) and explain the higher values of SPECT at day 4. It is also possible that one technique would be more sensitive than the other to mechanical damage of the vascular wall induced by the surgical procedure (Nagasawa and Kogure, 1989). Nevertheless, these small differences do not question the time course of changes in cerebral perfusion after MCAO.

Our results stand in good perspective with those of Lin *et al* (2008) who reported two successive phases of cerebral blood volume increase after MCAO: an early phase peaking at day 3 dependent of collateral circulation development and a late phase promoted by angiogenesis detected at day 7. They also observed an increase in the size of vessels with a diameter $> 30\,\mu$m on days 1 and 3, suggesting that the

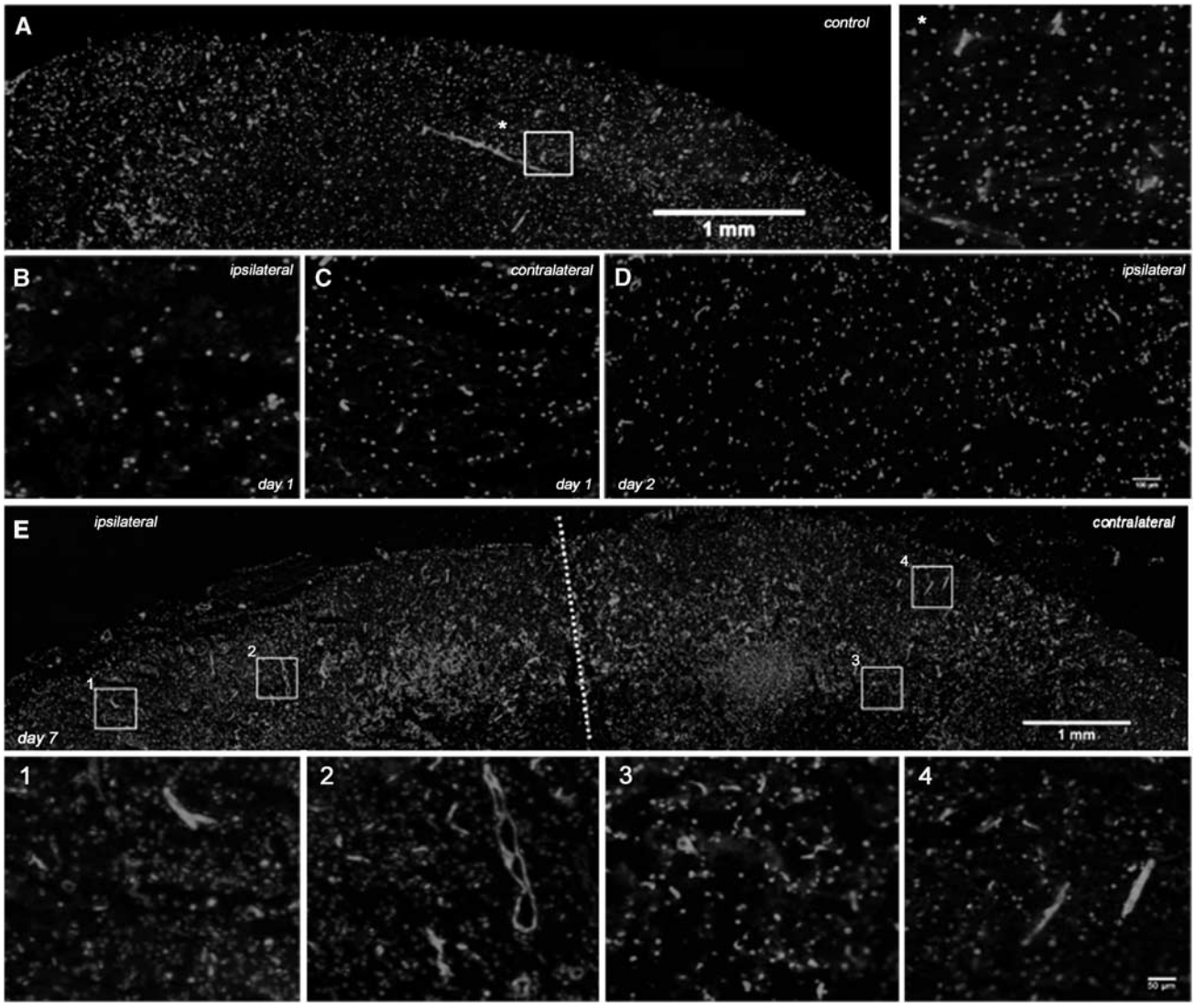

Figure 4 Evolution of CD31 expression in vessels after cerebral ischemia. Immunofluorescent labeling of CD31 (red) and DAPI (blue) in (**A**) the cerebral somatosensory cortex from a control brain, and after middle cerebral artery occlusion (MCAO) at day 1 in the ischemic area (**B**) and contralateral to lesion hemisphere (**C**), at day 2 in the ischemic side (**D**) and at day 7 in both hemispheres (**E**). Boxed areas and * in panel **A** and 1 to 4 in panel **E** are also shown at a higher magnification correspondingly. Boxed areas correspond to representative areas of cortical ischemic injury (1), surrounding area to the infarction (2), and contralateral hemisphere (3 and 4). The color reproduction of this figure is available at the *Journal of Cerebral Blood Flow and Metabolism* journal online.

early response to cerebral ischemia was a dilatation of blood vessels augmenting collateral circulation. Here, we analyzed by *ex-vivo* immunohistochemistry the vascular endothelial marker CD31 (PECAM-1), a cell adhesion molecule classically used to quantify microvessel density, at the same time points after reperfusion as those chosen for *in-vivo* imaging studies. CD31 density was similar in the ischemic area and normal brain tissue at day 1, but increased at days 2, 4, and 7. Since tissue perfusion is known to correlate with microvessel density (Gross *et al*, 1986), our results suggest that an increase in microvessel density, rather than vessel dilatation, is responsible for the return of perfusion to preischemic levels in the ischemic area. The initial increase in the diameter of preexisting blood vessels and collateral circulation appears to have little impact on perfusion, and angiogenesis appears as the major factor contributing to increasing blood supply to ischemic cerebral tissue.

Vascular Response in the Contralateral Area: Perfusion and Angiogenesis

The area of the brain contralateral to the MCAO was not directly concerned by the vessel occlusion but showed perfusion changes over time reminiscent of those found in the MCAO territory. There was a small reduction of the $[^{15}O]H_2O$ PET and $[^{99m}Tc]$HMPAO SPECT signals during occlusion and

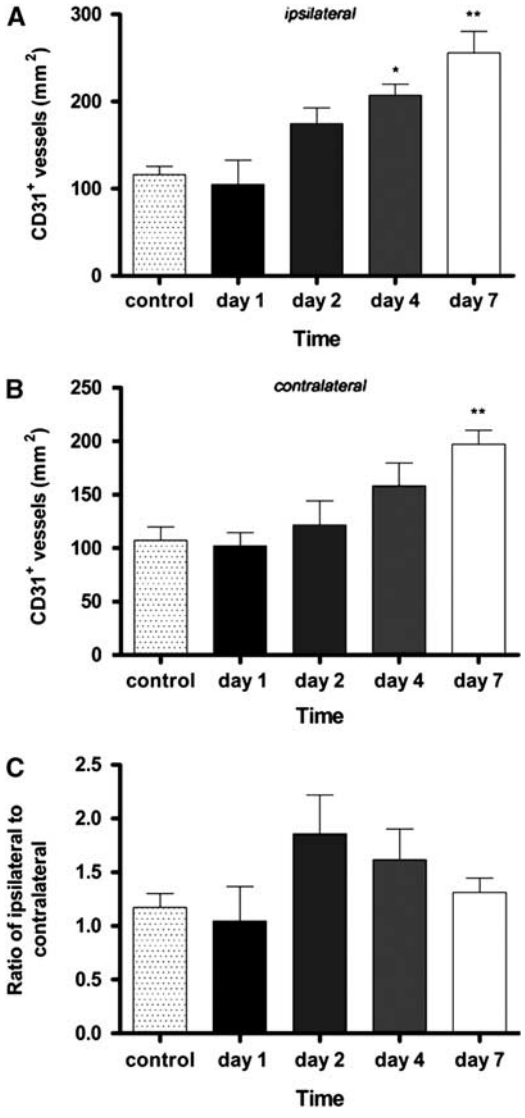

Figure 5 Time course of CD31 positive in ipsilateral (**A**), contralateral (**B**) hemispheres and ratio of the ipsilateral-to-contralateral (**C**) after cerebral ischemia. Statistically different from control: $*P < 0.05$, $**P < 0.01$.

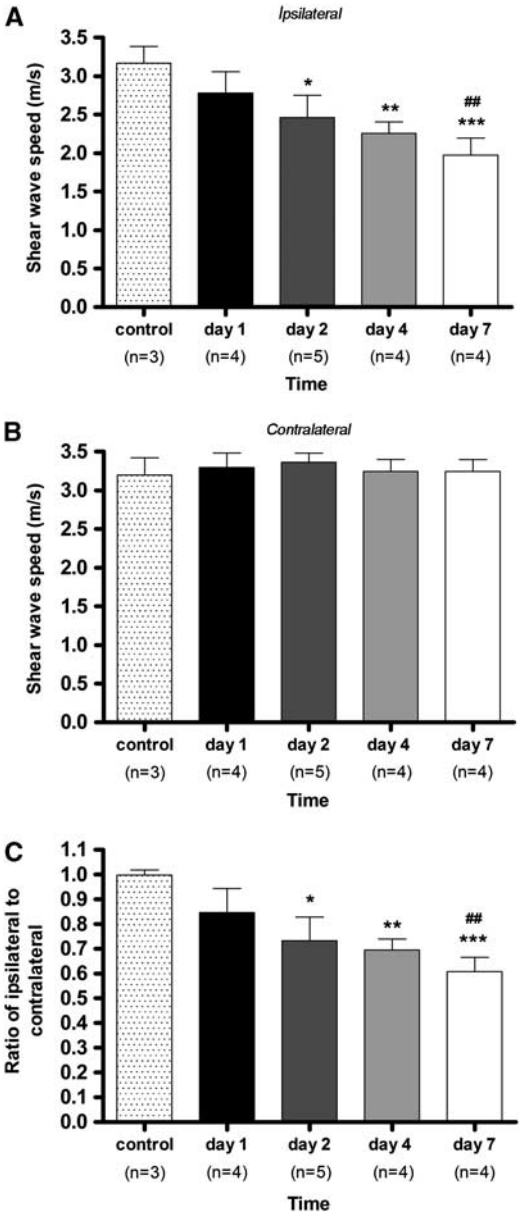

Figure 6 Evolution of tissue stiffness after cerebral ischemia in ipsilateral (**A**), contralateral (**B**) hemispheres and ratio of ipsilateral-to-contralateral (**C**) after cerebral ischemia. Statistically different from control: $*P < 0.05$, $**P < 0.01$, $***P < 0.001$. Statistically different from day 1: $^{\#\#}P < 0.01$.

at day 1, and an increase thereafter with a significant peak at 7 days after ischemia. Accordingly, the ratio of PET and SPECT signals in the ischemic to contralateral side varied from 0.5 to 0.6 at occlusion to 1.0 at days 4 to 7.

These results stand in contrast with those of a previous report that did not observe CBF increase after embolic cerebral ischemia affecting part of the striatum. However, in rats an increase of cortical CBF from days 3 to 7 after a proximal 1-hour MCAO was described by Lin *et al* (2002). Likewise, hyperperfusion in both cortex and caudate-putamen starting from day 3 after a distal 2-hour MCAO in rats has been also described (Wang *et al*, 2002). Taken together, the results from these four studies using different stroke models support the view that hyperperfusion in the brain contralateral to the lesion may be determined by the size and location of the ischemic injury.

Immunolabeling showed an increase in the number of CD31-positive vessels in the contralateral hemisphere at day 7 and our observation is consistent with a previous report of induction of angiogenesis-related genes in the contralateral cortex after a transient model of MCAO in rats (Cheung *et al*, 2000), and with the descriptions of increased new vessel formation in the ischemic boundary area after

ischemia (Beck and Plate, 2009). The increment of vessel density therefore appears to be responsible for increased perfusion, showed by [^{15}O]H_2O PET and [^{99m}Tc]HMPAO SPECT imaging, both in the ischemic area and in remote areas. It is tempting to hypothesize that this phenomenon is related to the remodeling or increased activity of neuronal circuits in the contralateral cortical hemisphere, which in turn could lead to improved functional recovery after cerebral ischemia (Takatsuru *et al*, 2009).

Cerebral Tissue Softening After Middle Cerebral Artery Occlusion

Brain softening (*ramollissement)* is the original hallmark of the consequence of ischemic stroke. However, information on the time course of cerebral tissue softening after stroke is scarce, even in rat models. The SWI is a novel imaging technique that allows assessing viscoelastic properties of the tissues and following the time course of brain softening after MCAO. The SWI acquisition provides quantitative maps of brain elasticity (described by Young's modulus E in kPa) based on the equivalent of a remote palpation of the brain (Bercoff *et al*, 2004). As the local shear wave speed Cs is directly linked to the local stiffness E (Cs = sqrt(E/3rho) where rho is the local density known to be quasi constant in soft tissues), the ultrasonic tracking of the shear wave propagation in the imaged plane yields a quantitative maps of local stiffness (either in Young's Modulus E in kPa or in Shear wave Speed Cs in m/s). The SWI is presently in clinical use for the exploration of suspect masses in peripheral tissues such as breast and liver (Muller *et al*, 2009; Tanter *et al*, 2008). Here, it was adapted to a spatial resolution compatible with the size of a rat brain, to yield quantitative maps of the internal elasticity and image their evolution after MCAO.

Interestingly, brain softening was a continuous process already present at day 1 after MCAO and increasing steadily up to day 7, a time at which the MCAO territory was 40% softer than normal brain tissue. In other words, brain elasticity decreased progressively and at least up to day 7. The continuous progress toward softer tissue indicates that softening begins early after stroke and suggests that it progresses independently of CBF or perfusion. This suggests that the softening of the brain is linked to a mechanical parameter of cerebral tissue rather than directly to perfusion or blood flow. The consequences of stroke are a loss of the architecture of the cerebral tissue and its necrotic liquefaction, but these mechanisms take place in the microstructure of the tissue and are not accessed directly by SWI, which measures the resulting changes in tissue elasticity at a macroscopic scale. An increased water concentration is likely to be present in edematous tissue and, even though water itself has no elasticity, the propagation of shear waves can be slowed by the presence of water inclusions smaller than the wavelength ($\lambda \approx 4$ mm) in brain tissue. As an example, it was observed in SWI maps of normal rat brains that the ventricles appear softer than the cerebral tissue (Macé *et al*, 2011). Alternatively, the destruction of the extracellular matrix will lead to disorganization of the tissue scaffold and increase tissue softness. In addition, stroke induces the release of angiogenic growth factors such as vascular endothelial growth factor (Leung *et al*, 1989) that has shown direct neuroprotectant effects on neurons in models of cerebral ischemia (Manoonkitiwongsa *et al*, 2004). Carmeliet (2003) described a relationship between vascular endothelial growth factor and increased leakiness of vessels, suggesting that both inflammation and vasogenic edema could be due to leakage from vessels facilitating the passage of inflammatory cells and liquid into the brain parenchyma (Croll *et al*, 2004). Among other causes, these mechanisms could explain the continuous progress toward softer tissue in the MCAO territory from day 1 to day 7 after cerebral ischemia in rats. At present, SWI cannot distinguish between these mechanisms and it cannot be excluded that, depending on the time after initial ischemia, different processes participate at varying levels to the changes in tissue elasticity. Nevertheless, it would be interesting to determine whether SWI can make early predictions on the evolution toward permanent lesions in animal models.

Finally, caution should be taken with regards to extrapolation of the present results concerning MCAO in rats to stroke in human patients. First, in rats a 2-hour transient MCAO induces irreversible permanent lesions; MCAOs of 25 minutes duration lead to long-term structural changes of brain parenchyma in two third of the cases (Garcia *et al*, 1997). The cerebral vasculature shows more redundancy and overlap between arterial territories in humans than in rodents and morphological, functional, and molecular changes of postischemic cerebral tissue depend on the level and duration of the reduction in blood flow (Khatri *et al*, 2009; Garcia *et al*, 1993). Hence, the time course of brain softening after stroke in humans remains to be determined. Second, at present a major limitation for brain SWI is the strong attenuation of ultrasound signals by the skull, requiring a cranial window. Research on alternative through-skull SWI methods is underway to adapt SWI to the human brain in clinical situations, at the moment limited in adult patients to intraoperative imaging during open-skull surgeries. However, SWI is directly applicable to newborns in a noninvasive manner through the fontanel window. It holds an important clinical potential in newborns, where it can be performed at the patient bedside with the same scanner and the same probe than standard sonography, providing information on tissue elasticity, which is not accessible by other modalities that could improve the diagnosis of several pathologies, including perinatal ischemia.

Summary and Conclusion

In summary, we show that a 2-hour transient MCAO in rats induces the formation of new vessels responsible for reperfusion and hyperperfusion over the whole brain, including the contralateral nonischemic areas. In parallel, the decrease of cerebral parenchyma elasticity, likely to reflect the loss of brain structural organization and function, is an early phenomenon progressing over time.

Acknowledgements

The authors are grateful to Drs Catherine Vuillemard, PharmD, Nicolas Tournier, PharmD, and Philippe Gervais, PharmD for help in formulation of the radiopharmaceuticals.

Disclosure/conflict of interest

The authors declare no conflict of interest.

References

Abercrombie J (1828) *Pathological and practical researches on diseases of the brain and spinal cord*. Edinburgh: Waugh and Innes

Allen CM (1984) Clinical diagnosis of stroke. *Lancet* 1:1357–8

Bercoff J, Pernot M, Tanter M, Fink M (2004) Monitoring thermally-induced lesions with supersonic shear imaging. *Ultrason Imaging* 26:71–84

Beck H, Plate KH (2009) Angiogenesis after cerebral ischemia. *Acta Neuropathol* 117:481–96

Bowler JV, Wade JP, Jones BE, Nijran KS, Steiner TJ (1998) Natural history of the spontaneous reperfusion of human cerebral infarcts as assessed by 99mTc HMPAO SPECT. *J Neurol Neurosurg Psychiatry* 64:90–7

Brea D, Sobrino T, Ramos-Cabrer P, Castillo J (2009) Inflammatory and neuroimmunomodulatory changes in acute cerebral ischemia. *Cerebrovasc Dis* 27:48–64

Bullock R, Statham P, Patterson J, Wyper D, Hadley D, Teasdale E (1990) The time course of vasogenic oedema after focal human head injury-evidence from SPECT mapping of blood brain barrier defects. *Acta Neurochir Suppl* 51:286–8

Carmeliet P (2003) Angiogenesis in health and disease. *Nat Med* 9:653–60

Cheung WM, Chen SF, Nian GM, Lin TN (2000) Induction of angiogenesis related genes in the contralateral cortex with a rat three-vessel occlusion model. *Chin J Physiol* 30:119–24

Couade M, Pernot M, Prada C, Messas E, Emmerich J, Bruneval P, Criton A, Fink M, Tanter M (2010) Quantitative assessment of arterial wall biomechanical properties using shear wave imaging. *Ultrasound Med Biol* 36:1662–76

Croll SD, Ransohoff RM, Cai N, Zhang Q, Martin FJ, Wei T, Kasselman LJ, Kintner J, Murphy AJ, Yancopoulos GD, Wiegand SJ (2004) VEGF-mediated inflammation precedes angiogenesis in adult brain. *Exp Neurol* 187: 388–402

Garcia JH, Liu KF, Ye ZR, Gutierrez JA (1997) Incomplete infarct and delayed neuronal death after transient middle cerebral artery occlusion in rats. *Stroke* 28:2303–9

Garcia JH, Yoshida Y, Chen H, Li Y, Zhang ZG, Lian J, Chen S, Chen S, Chopp M (1993) Progression from ischemic injury to infarct following middle cerebral artery in the rat. *Am J Pathol* 142:623–35

Granger CV, Hamilton BB, Fiedler RC (1992) Discharge outcome after stroke rehabilitation. *Stroke* 23:978–82

Gross PM, Sposito NM, Pettersen SE, Fenstermacher JD (1986) Differences in function and structure of the capillary endothelium in gray matter, white and a circumventricular organ of rat brain. *Blood Vessels* 23: 261–70

Heiss WD (2000) Ischemic penumbra: evidence from functional imaging in man. *J Cereb Blood Flow Metab* 20:1276–93

Heiss WD, Graf R, Wienhard K, Löttgen J, Saito R, Fujita T, Rosner G, Wagner R (1994) Dynamic penumbra demonstrated by sequential multitracer PET after middle cerebral artery occlusion in cats. *J Cereb Blood Flow Metab* 14:892–902

Khatri P, Abruzzo T, Yeatts SD, Nichols C, Broderick JP, Tomsick TA, IMS I and II Investigators (2009) Good clinical outcome after ischemic stroke with successful revascularization is time-dependent. *Neurology* 73: 1066–1072

Kuwabara Y, Ichiya Y, Sasaki M, Akashi Y, Yoshida T, Fukumura T, Masuda K (1996) Cerebellar vascular response to acetazolamide in crossed cerebellar diaschisis: a comparison of 99mTc-HMAPO single-photon emission tomography with 15-H2O positron emission tomography. *Eur J Nucl Med* 23:683–9

Latchaw RE, Yonas H, Hunter GJ, Yuh WT, Ueda T, Sorensen AG, Sunshine JL, Biller J, Wechsler L, Higashida R, Hademenos G (2003) Council on Cardiovascular Radiology of the American Heart Association. Guidelines and recommendations for perfusion imaging in cerebral ischemia: a scientific statement for healthcare. *Stroke* 34:1084–104

Leung DW, Cachianes G, Kuang WJ, Goeddel DV, Ferrara N (1989) Vascular endothelial growth factor is a secreted angiogenic mitogen. *Science* 246:1306–9

Lin CY, Chang C, Cheung WM, Lin MH, Chen JJ, Hsu CY, Chen JH, Lin TN (2008) Dynamic changes in vascular permeability, cerebral blood volume, vascular density, and size after transient focal cerebral ischemia in rats: evaluation with contrast-enhanced magnetic resonance imaging. *J Cereb Blood Flow Metab* 28:1491–501

Lin TN, Sun SW, Cheung WM, Li F, Chang C (2002) Dynamic changes in cerebral blood flow and angiogenesis after transient focal cerebral ischemia in rats. Evaluation with serial magnetic resonance imaging. *Stroke* 33:2985–91

Liu F, McCullough LD (2011) Middle cerebral artery occlusion model in rodents: Methods and potential pitfalls. *J Biomed Biotechnol* 2011:464701

Lopez AD, Mathers CD, Ezzati M, Jamison DT, Murray CJ (2006) Global and regional burden of disease and risk factors, 2001: systematic analysis of population health data. *Lancet* 367:1747–57

Macé E, Montaldo G, Cohen I, Baulac M, Fink M, Tanter M (2011) Functional ultrasound imaging of the brain. *Nat Methods* 8:662–4

Manoonkitiwongsa PS, Schultz RL, McCreery DB, Whitter EF, Lyden PD (2004) Neuroprotection of ischemic brain by vascular endothelial growth factor is critically

dependent on proper dosage and may be compromised by angiogenesis. *J Cereb Blood Flow Metab* 24:693–702
Martín A, Boisgard R, Kassiou M, Dollé F, Tavitian B (2011) Reduced PBR/TSPO expression after minocycline treatment in a rat model of focal cerebral ischemia: a PET study using [(18)F]DPA-714. *Mol Imaging Biol* 13:10–5
Martín A, Boisgard R, Thézé B, Van Camp N, Kunhast B, Damont A, Kassiou M, Dollé F, Tavitian B (2010) Evaluation of the PBR/TSPO radioligand [(18)F]DPA-714 in a rat model of focal cerebral ischemia. *J Cereb Blood Flow Metab* 30:230–41
Muller M, Gennisson JL, Deffieux T, Tanter M, Fink M (2009) Quantitative viscoelasticity mapping of human liver using supersonic shear imaging: preliminary *in vivo* feasibility study. *Ultrasound Med Biol* 35:219–29
Nagasawa H, Kogure K (1989) Correlation between cerebral blood flow and histologic changes in a new rat model of middle cerebral artery occlusion. *Stroke* 20:1037–43
Pappata S, Fiorelli M, Rommel T, Hartmann A, Dettmers C, Yamaguchi T, Chabriat H, Poline JB, Crouzel C, Di Giamberardino L (1993) PET study of changes in local brain hemodynamics and oxygen metabolism after unilateral middle cerebral artery occlusion in baboons. *J Cereb Blood Flow Metab* 13:416–24
Plate KH (1999) Mechanisms of angiogenesis in the brain. *J Neuropathol Exp Neurol* 58:313–20
Rojas S, Martín A, Pareto D, Herance JR, Abad S, Ruíz A, Flotats N, Gispert JD, Llop J, Gómez-Vallejo V, Planas AM (2011) Positron emission tomography with ^{11}C-flumazenil in the rat shows preservation of binding sites during the acute phase after 2h-transient focal ischemia. *Neuroscience* 182:208–16
Rostan L (1823) *Recherches sur le ramollissement du cerveau; ouvrage dans lequel on s'efforce de distinguer les diverses affections de ce viscère par des signes caractéristiques*. 2nd edn. Paris: Béchet Jeune
Schweinhardt P, Fransson P, Olson L, Spenger C, Andersson JL (2003) A template for spatial normalisation of MR images of the rat brain. *J Neurosci Methods* 129:105–13
Singer OC, Humpich MC, Fiehler J, Albers GW, Lansberg MG, Kastrup A, Rovira A, Liebeskind DS, Gass A, Rosso C, Derex L, Kim JS, Neumann-Haefelin T, MR Stroke Study Group Investigators (2008) Risk for symptomatic intracerebral hemorrhage after thrombolysis assessed by diffusion-weighted magnetic resonance imaging. *Ann Neurol* 63:52–60
Sperling B, Lassen NA (1993) Hyperfixation of HMPAO in subacute ischemic stroke leading to spuriously high estimates of cerebral blood flow by SPECT. *Stroke* 24: 193–4
Takatsuru Y, Fukumoto D, Yoshitomo M, Nemoto T, Tsukada H, Nabekura J (2009) Neuronal circuit remodeling in the contralateral cortical hemisphere during functional recovery from cerebral infarction. *J Neurosci* 29:10081–6
Tanter M, Bercoff J, Athanasiou A, Deffieux T, Gennisson JL, Montaldo G, Muller M, Tardivon A, Fink M (2008) Quantitative assessment of breast lesion viscoelasticity: initial clinical results using supersonic shear imaging. *Ultrasound Med Biol* 34:1373–86
Thiel A, Heiss WD (2011) Imaging of microglia activation in stroke. *Stroke* 42:507–12
Treger I, Streifler JY, Ring H (2005) The relationship between mean flow velocity and functional and neurological parameters of ischemic stroke patients undergoing rehabilitation. *Arch Phys Med Rehabil* 86:427–30
Ueda T, Hatakeyama T, Kumon Y, Sakaki S, Uraoka T (1994) Evaluation of risk of hemorrhagic transformation in local intra-arterial thrombolysis in acute ischemic stroke by initial SPECT. *Stroke* 25:298–303
Umemura A, Suzuka T, Yamada K (2000) Quantitative measurement of cerebral blood flow by (99m)Tc-HMPAO SPECT in acute ischaemic stroke: usefulness in determining therapeutic options. *J Neurol Neurosurg Psychiatry* 69:472–8
Wang L, Yushmanov VE, Liachenko SM, Tang P, Hamilton RL, Xu Y (2002) Late reversal of cerebral perfusion and water diffusion after transient focal ischemia in rats. *J Cereb Blood Flow Metab* 22:253–61
Wintermark M (2005) Brain perfusion-CT in acute stroke patients. *Eur Radiol* 15:28–31